Ammonia-Induced Structural Changes of the Oxygen-Evolving Complex in Photosystem II As Revealed by Light-Induced FTIR Difference Spectroscopy †

ARTICLE *in* BIOCHEMISTRY · AUGUST 2004

Impact Factor: 3.02 · DOI: 10.1021/bi0499260 · Source: PubMed

5 AUTHORS, INCLUDING:

Hsiu-An Chu
Academia Sinica
30 PUBLICATIONS **1,087** CITATIONS

SEE PROFILE

Ammonia-Induced Structural Changes of the Oxygen-Evolving Complex in Photosystem II As Revealed by Light-Induced FTIR Difference Spectroscopy†

Hsiu-An Chu,*,‡ Ya-Wen Feng,‡ Chiu-Ming Wang,‡ Kuo-An Chiang,§ and Shyue-Chu Ke*,§

Institute of Botany, Academia Sinica, Taipei, Taiwan 11529, Republic of China, and Department of Physics, National Dong Hwa University, Hualien, Taiwan 974-01, Republic of China

Received January 9, 2004; Revised Manuscript Received June 25, 2004

ABSTRACT: Light-induced Fourier transform infrared difference spectroscopy has been applied to studies of ammonia effects on the oxygen-evolving complex (OEC) of photosystem II (PSII). We found that NH_3 induced characteristic spectral changes in the region of the symmetric carboxylate stretching modes (1450−1300 cm^{-1}) of the $S_2Q_A^-/S_1Q_A$ FTIR difference spectra of PSII. The S_2 state carboxylate mode at 1365 cm^{-1} in the $S_2Q_A^-/S_1Q_A$ spectrum of the controlled samples was very likely upshifted to 1379 cm^{-1} in that of NH_3-treated samples; however, the frequency of the corresponding S_1 carboxylate mode at 1402 cm^{-1} in the same spectrum was not significantly affected. These two carboxylate modes have been assigned to a Mn-ligating carboxylate whose coordination mode changes from bridging or chelating to unidentate ligation during the S_1 to S_2 transition [Noguchi, T., Ono, T., and Inoue, Y. (1995) *Biochim. Biophys. Acta 1228*, 189−200; Kimura, Y., and Ono, T.-A. (2001) *Biochemistry 40*, 14061−14068]. Therefore, our results show that NH_3 induced significant structural changes of the OEC in the S_2 state. In addition, our results also indicated that the NH_3-induced spectral changes of the $S_2Q_A^-/S_1Q_A$ spectrum of PSII are dependent on the temperature of the FTIR measurement. Among the temperatures we measured, the strongest effect was seen at 250 K, a lesser effect was seen at 225 K, and little or no effect was seen at 200 K. Furthermore, our results also showed that the NH_3 effects on the $S_2Q_A^-/S_1Q_A$ spectrum of PSII are dependent on the concentrations of NH_4Cl. The NH_3-induced upshift of the 1365 cm^{-1} mode is apparent at 5 mM NH_4Cl and is completely saturated at 100 mM NH_4Cl concentration. Finally, we found that CH_3NH_2 has a small but clear effect on the spectral change of the $S_2Q_A^-/S_1Q_A$ FTIR difference spectrum of PSII. The effects of amines on the $S_2Q_A^-/S_1Q_A$ FTIR difference spectra (NH_3 > CH_3NH_2 > AEPD and Tris) are inverse proportional to their size (Tris ∼ AEPD > CH_3NH_2 > NH_3). Therefore, our results showed that the effects of amines on the $S_2Q_A^-/S_1Q_A$ spectrum of PSII are sterically selective for small amines. On the basis of the correlations between the conditions (dependences on the excitation temperature and NH_3 concentration and the steric requirement for the amine effects) that give rise to the NH_3-induced upshift of the 1365 cm^{-1} mode in the $S_2Q_A^-/S_1Q_A$ spectrum of PSII and the conditions that give rise to the altered S_2 state multiline EPR signal, we propose that the NH_3-induced upshift of the 1365 cm^{-1} mode is caused by the binding of NH_3 to the site on the Mn cluster that gives rise to the altered S_2 state multiline EPR signal. In addition, we found no significant NH_3-induced change in the $S_2Q_A^-/S_1Q_A$ FTIR difference spectrum at 200 K. Under this condition, the OEC gives rise to the NH_3-stabilized $g = 4.1$ EPR signal and a suppressed $g = 2$ multiline EPR signal. Our results suggest that the structural difference of the OEC between the normal $g = 2$ multiline form and the NH_3-stabilized $g = 4.1$ form is small.

The catalytic site of photosynthetic oxygen evolution contains a tetranuclear Mn cluster that interacts closely with a redox-active tyrosine residue known as Y_Z. Ca^{2+} and Cl^- are essential cofactors (for review see refs *1*−*4*). The Mn cluster accumulates oxidizing equivalents in response to photoinduced electron transfer reactions within PSII[1] and then catalyzes the oxidation of two molecules of water, consequently releasing one molecule of O_2 as a byproduct. The progression of the OEC goes through a cycle of five intermediate states, labeled as the S_n state ($n = 0-4$), where n denotes the number of stored equivalents. The S_1 state is predominated in the dark-adapted samples; in the S_4 state, water is split, O_2 is released, and the OEC returns to the S_0

† This work was supported by the National Science Council in Taiwan (NSC 92-2311-B-001-054) and by Academia Sinica to H.-A.C. and by the National Science Council in Taiwan (NSC 92-2112-M-259-008) to S.-C.K.

* To whom correspondence should be addressed. H.-A.C.: phone, 886-2-27899590 ext 308; fax, 886-2-27827954; e-mail, chuha@gate.sinica.edu.tw. S.-C.K.: phone, 886-3-8633705; fax, 886-3-8633690; e-mail, ke@mail.ndhu.edu.tw.

‡ Academia Sinica.

§ National Dong Hwa University.

[1] Abbreviations: AEPD, 2-amino-2-ethyl-1,3-propanediol; CH_3NH_2, methylamine; DCMU, 3-(3,4-dichlorophenyl)-1,1-dimethylurea; EPR, electron paramagnetic resonance; ESE, electron spin−echo; ESEEM, electron spin−echo envelope modulation; EXAFS, extended X-ray absorption fine structure; FTIR, Fourier transform infrared; HEPES, *N*-(2-hydroxyethyl)piperazine-*N*′-2-ethanesulfonic acid; MES, 2-(*N*-morpholino)ethanesulfonic acid; OEC, oxygen-evolving complex; OTG, octyl β-D-thioglucopyranoside; PSII, photosystem II; Q_A, the primary quinone electron acceptor in PSII.

10.1021/bi0499260 CCC: $27.50
Published on Web 00/00/0000 PAGE EST: 8.6

state (*5*, *6*). Recent X-ray crystal structures of PSII were determined to be about 3.7 Å resolution (*7*, *8*). In these new structures of PSII, the general shape and location of the OEC in PSII are determined. However, the detailed molecular structure and ligation of the PSII/OEC are not yet observable.

NH_3 is a structural analogue of substrate H_2O and an inhibitor to the water oxidation reaction in PSII (for reviews see refs *9* and *10*). Steady-state inhibition studies by Sandusky and Yocum described two independent sites for ammonia inhibition of oxygen evolution and named them "SY I" and "SY II" (*11*, *12*). The SY I site showed inhibition by the class of amines (NH_3, Tris, methylamine, 2-amino-2-ethylpropanediol, and *tert*-butylamine) that are competitive with Cl^-. The SY II site was accessible only to NH_3, and the NH_3 binding was not competitive with respect to Cl^-.

EPR studies demonstrated that no alternations of the S_2 state multiline EPR signal are observed when samples that are poised in the dark-stable S_1 state are illuminated at 200 K but that alternations are produced when samples that have been illuminated at 200 K are subsequently "annealed" at 273 K or when samples that are poised in the dark-stable S_1 state are illuminated at 273 K (*13*). These results were interpreted as showing that coordination of NH_3 to the Mn site occurs after formation of the S_2 state (*13*−*15*). Comparison of ^2H ESE modulation in control and ammonia-treated samples incubated in ^2H_2O supported the idea that NH_3 displaced a water ligand upon binding to Mn in this NH_3-specific (type II) site (*16*). ESEEM experiments performed on the NH_3-altered multiline EPR signals using both $^{14}NH_3$ and $^{15}NH_3$ concluded that a single NH_3-derived ligand binds directly to the Mn cluster in the S_2 state (*17*). In addition, analysis of the ^{14}N quadrupolar interaction provided evidence in favor of an amido (NH_2) bridge formed between Mn ions. Changes in multiline EPR line shapes were interpreted as the result of a change in the overall pattern of magnetic exchange interactions within the cluster caused by the formation of this new bridge (*17*). An EXAFS study under the condition of NH_3-altered multiline EPR signals reported an increase in one 2.7 Å Mn−Mn distance by 0.15 Å whereas the Mn−Mn distance of the second unit seem to be unaffected by ammonia treatment (*18*). This result was interpreted as the elongation of one Mn di-μ-oxo core of the OEC, probably due to the replacement of one bridging μ-oxo in this core with an amido (NH_2) group. In addition, this EXAFS study showed that there were only small effects on position, shape, and orientation dependence on the Mn K-edge spectra result from ammonia treatment. These results indicated that the Mn oxidation state, the symmetry of the Mn ligand environment, and the orientation of the Mn complex remain essentially unaffected in the annealed NH_3 S_2 state (*18*).

One EPR study probed the nature of the ligand-binding site on the Mn cluster in PSII by monitoring the S_2 state multiline EPR spectrum in the presence of several primary amines (*14*). This study showed that amines other than NH_3 (Tris, AEPD, CH_3NH_2) do not affect the hyperfine line pattern and temperature dependence of the S_2 state multiline EPR signal. The authors of this study concluded that amines other than NH_3 do not readily bind to this Mn site in the S_2 state because of the steric factors (*14*).

Additional EPR studies showed that NH_3 stabilizes the $g = 4$ signal relative to the $g = 2$ multiline signal upon illumination at 200 K (*14*, *19*−*21*). These observations were interpreted as demonstrating that the binding of NH_3 to an additional site, probably the Cl^- site, on the OEC occurred already in the S_1 state (*14*). The NH_3-stabilized $g = 4$ signal obtained in oriented PSII membranes displayed at least 16 partially resolved Mn hyperfine transitions with a regular spacing of 36 G (*22*, *23*). The partially resolved hyperfine structure provided unambiguous evidence for a tetranuclear Mn origin for the $g = 4$ signal (*22*, *23*). However, it is not clear whether NH_3 binding at this site represents direct ligation to the Mn cluster or binding to a site in close proximity to the Mn cluster. The structure of this Cl^- competitive, NH_3-binding site is less well characterized than the Cl^--insensitive, NH_3-specific site on the OEC, presumably due to the relative difficulty of performing ENDOR or ESEEM spectroscopy on the high-spin $g = 4.1$ EPR signal (*17*).

Light-induced FTIR difference spectroscopy has been extensively applied to study structural changes of the OEC during the S state transitions. These structural changes include the protein and ligand environment around the OEC (*24*−*38*), the structure and bonding of the Mn cluster (*39*−*43*), and active water molecules interacting with the OEC (*44*, *45*). Several carboxylate stretching modes and one histidine mode have been identified in the midfrequency (1000−2000 cm^{-1}) S_2/S_1 FTIR difference spectrum of intact PSII samples (*24*−*38*). Previous research has proposed that these carboxylate and histidine modes originate from carboxylate and histidine ligands of the OEC that undergo structural changes during the S_1 to S_2 transition (*24*−*38*). Negative bands at ∼1560 and ∼1402 cm^{-1} and positive bands at ∼1588 and ∼1364 cm^{-1} have been assigned to an Mn-ligating carboxylate whose coordination mode changes from bridging or chelating to unidentate ligation during the S_1 to S_2 transition (*24*, *32*). A negative band at ∼1561 cm^{-1} has been assigned to the asymmetric stretching mode of a carboxylate group that forms a hydrogen bond with a Mn-bound water molecule (*25*). Site-directed mutagenesis (*2*) and the recent X-ray crystal structures of PSII (*7*, *8*) suggest that the D1 polypeptide provides most, if not all, of the protein ligands to the Mn cluster. In combination with site-directed mutagenesis and isotopic labeling, FTIR difference spectroscopy has been applied to identify the amino acid origin of these carboxylate modes in the S_2/S_1 FTIR difference spectrum of PSII (*37*, *38*). One such study showed that D1-Asp170 is structurally coupled to the Mn cluster during the S_1 to S_2 transition but that this residue is not the origin of carboxylate modes at ∼1402 and at ∼1364 cm^{-1} in the S_2/S_1 FTIR difference spectrum of PSII (*37*). Another such study showed that a negative band at ∼1356 cm^{-1} and a positive band at ∼1339 or ∼1320 cm^{-1} in S_2/S_1 FTIR difference spectrum of PSII originate from the symmetric stretching mode of the α-COO^- of Ala344 at the C-terminus of the D1 polypeptide (*38*). These frequencies are consistent with unidentate ligation of the Mn cluster by the α-COO^- group of D1-Ala344 in both the S_1 and S_2 states (*38*). FTIR difference spectroscopy has also been applied to study the effects of the calcium and chloride cofactors on the structure and mechanism of the OEC in PSII (*24*, *33*, *34*). However, this FTIR difference technique has not yet been applied to study the effects of NH_3 on the OEC.

In this study, the effects of NH_3 on the $S_2Q_A^-/S_1Q_A$ FTIR difference spectrum of PSII have been examined in order to obtain structural information about ammonia coordination to the catalytic site of the OEC during the S_1 to S_2 transition. In addition, the properties of NH_3-binding sites on the PSII/OEC are also discussed.

MATERIALS AND METHODS

Sample Conditions for FTIR Measurement. Spinach OTG PSII reaction center cores (RCCs), retaining the three extrinsic polypeptides, were prepared as described in ref *46*. Typical oxygen evolution rates were about 1.1−1.4 mmol of O_2 (mg of Chl)$^{-1}$ h^{-1}. NH_4Cl- and amine-treated PSII samples were prepared from PSII OTG RCCs. These RCCs were washed twice with HEPES buffer (40 mM HEPES, 10 mM NaCl, 0.4 M sucrose at pH 7.5). Either $^{14}NH_4Cl$ or $^{15}NH_4Cl$ or other amines (CH_3NH_2, AEPD, and Tris) were added from a 1.25 M stock solution (pH was adjusted to pH 7.5) to a final concentration of 100 mM or to the concentration as indicated in the text. For controlled PSII samples, the same concentration of NaCl was added in place of NH_4Cl. The sample suspension included 0.1 mM DCMU for the $S_2Q_A^-/S_1Q_A$ FTIR difference spectrum or 0.1 mM DCMU and 10 mM NH_2OH for the Q_A^-/Q_A difference spectrum. DCMU was added from 10 mM solution in 95% ethanol. NH_2OH was added from 1 M solution (pH was adjusted to pH 7.5) prepared just before it was used. NH_2OH were added as an exogenous electron donor. Samples for FTIR measurement were prepared by centrifuging PSII OTG cores (15 min at 20000 rpm) to produce a pellet that was then sandwiched between two CaF_2 sample windows. $^{15}NH_4Cl$ with 98+ atom % ^{15}N was purchased from Aldrich Chemical Co.

Experimental Conditions for FTIR Measurement. Mid-frequency FTIR experiments were performed on a Bruker EQUINOX 55 spectrometer that was equipped with a KBr beam splitter and a photovoltaic MCT detector. Samples were cooled to 250 K by using an Oxford DN liquid nitrogen cryostat. The sample temperature was regulated to ±0.1 K with a temperature controller (Oxford ITC 502). Samples were illuminated for 4 s by a Dolan-Jenner MI 150 high-intensity illuminator with a heat filter and a low-frequency filter that passes visible light >650 nm. Double-sided forward−backward interferograms were recorded with a scanner velocity of 60 kHz. For the calculation of Fourier transforms, a Blackmann−Harris three-term apodization function and a zero-filled factor of 4 were employed. The acquisition time for all spectra was 1 min (387 scans). The light-minus-dark FTIR difference spectrum was calculated from the ratio of the single-beam dark spectrum and that following illumination. The spectral resolution for all spectra was 4 cm^{-1}. The S_2/S_1 difference spectrum was obtained by subtracting the Q_A^-/Q_A difference spectrum from the $S_2Q_A^-/S_1Q_A$ difference spectrum (*24*, *32*, *34*). The multiple difference spectra were averaged to improve the signal to noise ratio of the spectra.

Conditions for EPR Measurements. EPR control experiments were performed on pellets of PSII OTG core samples in the similar manner as for FTIR samples. In the final centrifugation step, the EPR samples were prepared by centrifuging PSII OTG cores (25 min at 5880*g*) to produce a pellet in EPR tubes. The samples were illuminated for 1.5 min in a nonsilvered Dewar in a cold ethanol bath at 250 K by the addition of dry ice. The samples were frozen in liquid nitrogen after illumination. EPR spectra were obtained at X-band using a Bruker EMX spectrometer equipped with a Bruker TE102 cavity and an Advanced Research System continuous-flow cryostat (3.2−200 K). The microwave frequency was measured with a Hewlett-Packard 5246L electronic counter. The instrument settings are shown in the figure legend.

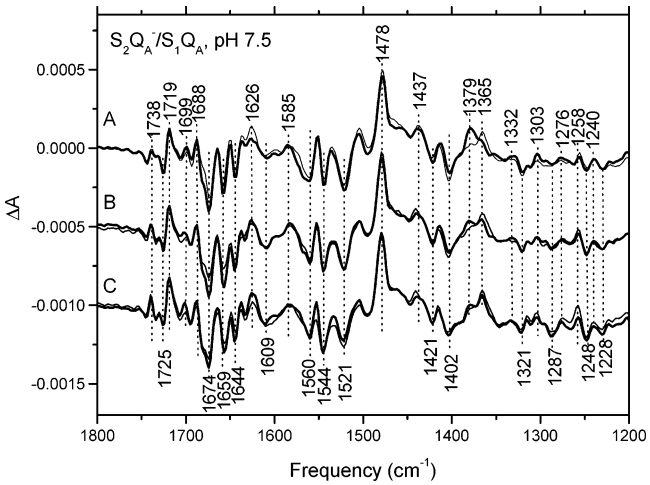

FIGURE 1: Temperature dependence of $S_2Q_A^-/S_1Q_A$ FTIR difference spectra of NH_3-treated (thick line) and controlled (thin line) PSII samples. The spectra were recorded at (A) 250 K, (B) 225 K, and (C) 200 K, respectively. The PSII samples were treated with 100 mM NH_4Cl or 100 mM NaCl (control). The sample suspension also included 0.1 mM DCMU. These spectra represent the averages of eight to ten, five, and four difference spectra, respectively. The intensity of each spectrum has been normalized with respect to the Q_A^- band at 1478 cm^{-1}.

RESULTS

Ammonia-Induced Changes on $S_2Q_A^-/S_1Q_A$ FTIR Difference Spectra of PSII. Previous EPR studies demonstrated that the appearance of the NH_3-modified S_2 state $g = 2$ multiline EPR signal is dependent on the temperature of illumination (*13*). The modified S_2 state multiline EPR signal is generated when NH_3-treated (100 mM NH_4Cl, pH 7.5) PSII samples are illuminated above 250 K but is not generated when samples are illuminated at 200 K. We expect that the possible effects of NH_3 on the light-induced $S_2Q_A^-/S_1Q_A$ FTIR difference spectrum will show a similar temperature-dependent behavior. Therefore, we performed light-induced $S_2Q_A^-/S_1Q_A$ FTIR difference measurements on NH_3-treated (100 mM NH_4Cl, pH 7.5) and controlled (100 mM NaCl, pH 7.5) PSII samples at three temperatures (200, 225, and 250 K) in order to identify possible NH_3-induced spectral changes. The results are shown in Figure 1. Indeed, we found that NH_3 altered the spectral region (1450−1300 cm^{-1}) of the symmetric carboxylate stretching modes in the $S_2Q_A^-/S_1Q_A$ FTIR difference spectrum of PSII at 250 K. The 1365/1402 cm^{-1} bands in the $S_2Q_A^-/S_1Q_A$ FTIR difference spectrum of controlled PSII samples have been assigned by previous FTIR studies to symmetric carboxylate stretching modes that are shifted during the S_2/S_1 transition (*24*). We found that the intensity of the S_2 symmetric carboxylate mode at 1365 cm^{-1} was progressively diminished and a new mode appeared in the $S_2Q_A^-/S_1Q_A$ spectrum of NH_3-treated PSII

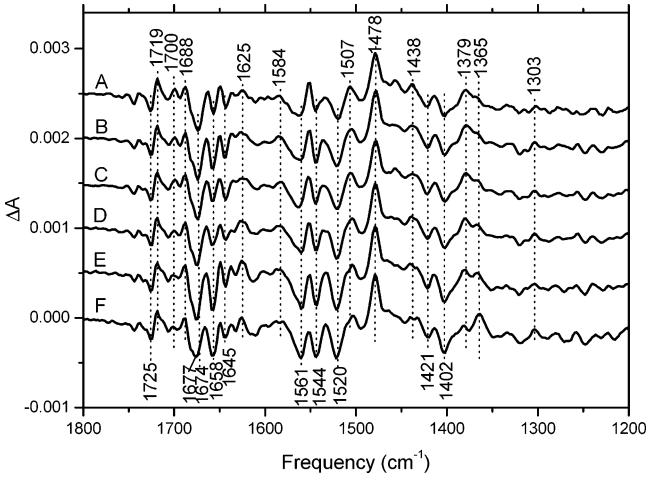

FIGURE 2: Effect of increasing concentrations of NH_4Cl on the changes of $S_2Q_A^-/S_1Q_A$ spectra of NH_3-treated PSII. The spectra were recorded at 250 K. The PSII samples were treated with (A) 200 mM, (B) 100 mM, (C) 50 mM, (D) 10 mM, (E) 5 mM, and (F) no addition of NH_4Cl, respectively. Each $S_2Q_A^-/S_1Q_A$ spectrum is the average of difference spectra from four different samples, except spectrum B is the average of ten difference spectra. The sample suspension also included 0.1 mM DCMU. The intensity of each spectrum has been normalized with respect to the Q_A^- band at 1478 cm^{-1}.

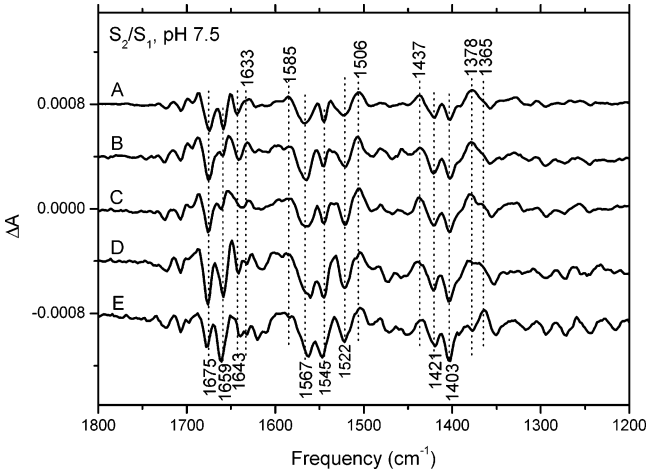

FIGURE 3: Effect of increasing concentrations of NH_4Cl on the changes of the double-difference S_2/S_1 spectra of NH_3-treated PSII. The spectra were recorded at 250 K. The PSII samples were treated with (A) 100 mM, (B) 50 mM, (C) 10 mM, (D) 5 mM, and (E) no addition of NH_4Cl, respectively. Each S_2/S_1 spectrum was obtained by subtracting the light-induced Q_A^-/Q_A difference spectrum from the light-minus-dark $S_2Q_A^-/S_1Q_A$ FTIR difference spectrum of PSII samples. The sample suspension included 0.1 mM DCMU for the $S_2Q_A^-/S_1Q_A$ FTIR difference spectrum or 0.1 mM DCMU and 10 mM NH_2OH for the Q_A^-/Q_A difference spectrum. The intensity of each spectrum has been normalized with respect to the Q_A^- band at 1478 cm^{-1}.

at ~1379 cm^{-1} as the temperature of the measurement increased from 200 to 250 K. When the FTIR measurement was performed at or above 265 K, the amplitude of the $S_2Q_A^-/S_1Q_A$ spectrum diminished significantly owing to rapid charge recombination of the $S_2Q_A^-$ state (data not shown). In this study, we used PSII OTG core samples, which gave 2−3-fold larger FTIR signals than PSII-enriched membranes under our experimental conditions, while maintaining their functional integrity to a significant extent. We found that the temperature dependence of the NH_3-induced FTIR spectral changes (e.g., upshift of the 1365 cm^{-1} mode) in the $S_2Q_A^-/S_1Q_A$ FTIR difference spectrum in BBY PSII-enriched membranes are identical to that in the PSII OTG core in Figure 1. Furthermore, the spectrum and the dependence of the exciting temperature of the NH_3-modified $g = 2$ multiline EPR signal in the PSII OTG core is very similar to those in BBY PSII-enriched membranes (data not shown). Therefore, our results showed that the temperature dependence of this NH_3-induced FTIR spectral change (e.g., upshift of the 1365 cm^{-1} mode) in the $S_2Q_A^-/S_1Q_A$ FTIR difference spectrum is very similar to that of the formation of the NH_3-modified $g = 2$ multiline EPR signal.

Figures 2 and 3 show the effect of increasing concentrations of NH_4Cl on the changes of the $S_2Q_A^-/S_1Q_A$ and the double-difference S_2/S_1 FTIR difference spectra of NH_3-treated PSII, respectively. The double-difference S_2/S_1 FTIR difference spectra were obtained by subtracting the Q_A^-/Q_A FTIR difference spectrum from the $S_2Q_A^-/S_1Q_A$ FTIR difference spectrum of PSII samples (*24*, *32*, *34*). The intensity of the S_2 carboxylate mode at 1365 cm^{-1} progressively decreased and the intensity of the positive mode at about ~1379 cm^{-1} progressively increased in Figures 2 and 3 as the concentration of NH_4Cl increased from 0 to 100 mM. In addition, the NH_3 effect is apparent at 5 mM NH_4Cl and completely saturated at 100 mM NH_4Cl concentration. Furthermore, we found that the dependence on the NH_4Cl concentration for the NH_3-induced FTIR spectral changes (e.g., upshift of the 1365 cm^{-1} mode) in the $S_2Q_A^-/S_1Q_A$ FTIR difference spectrum in BBY PSII-enriched membranes is very similar to that in PSII OTG cores as in Figure 2 (data not shown). Previous EPR studies have shown that, at 10 mM NH_4Cl concentration, a modified $g = 2$ multiline and a $g = 4.2$ EPR signal were generated when samples that were poised in the dark-stable S_1 state were illuminated at 273 or 253 K (*19*−*21*). In addition, one EPR study estimated that the apparent dissociation constant for the ammonia-binding site of the OEC that gives rise to the $g = 2$ modified EPR signal is about 3 mM NH_4^+ concentration (*20*). Furthermore, previous EPR studies also showed that the formation of the modified multiline signal appeared to increase with NH_4Cl concentration (*20*, *21*). Figure 4 shows the effect of increasing concentrations of NH_4Cl on the S_2 state EPR signals generated in PSII OTG core samples by illumination at 250 K. Our EPR results showed that, at 5 mM NH_4Cl concentration, the $g = 2$ multiline EPR signal was modified and a $g = 4.2$ EPR signal was also generated when samples that were poised in the dark-stable S_1 state were illuminated at 250 K. The average of the hyperfine line spacing for the modified (Figure 4A−C) and normal (Figure 4D) $g = 2$ multiline EPR signal is about 69 and 85 G, respectively. In addition, the formation of the modified multiline EPR signal appeared to increase with NH_4Cl concentration, and its concentration dependence was generally correlated with that of the NH_3-induced FTIR spectral changes (e.g., upshift of the 1365 cm^{-1} mode). The intensity of the $g = 4.2$ signal was progressively diminished as NH_4Cl concentration increased from 5 to 100 mM in Figure 4.

A simple explanation for the above FTIR results is that the symmetric carboxylate stretching mode that appears at 1365 cm^{-1} in the $S_2Q_A^-/S_1Q_A$ spectrum is upshifted to 1379 cm^{-1} upon treatment with NH_3. Alternatively, it is possible that the spectral change might be caused by the absorption from other species. For example, an NH_3-derived species

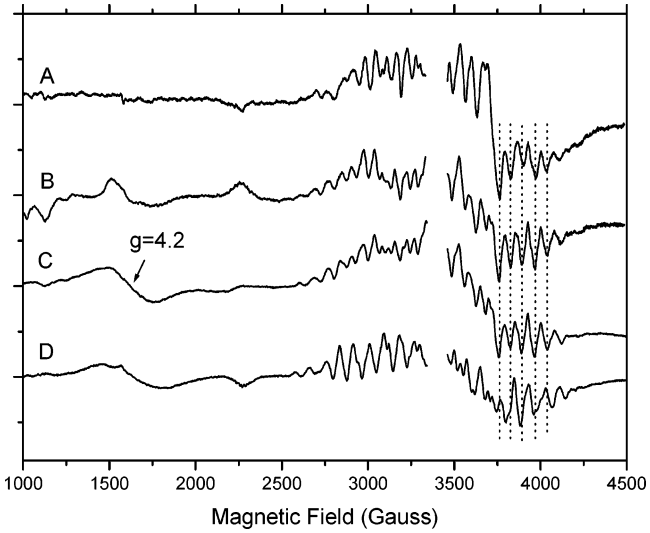

FIGURE 4: Dependence on the NH_4Cl concentration of the S_2 state EPR spectra generated in PSII OTG core samples by illumination at 250 K. The PSII samples were treated with (A) 100 mM, (B) 10 mM, (C) 5 mM, and (D) no addition of NH_4Cl, respectively. Instrument settings: microwave frequency, 9.51 GHz; modulation amplitude, 20 G at 100 kHz; temperature, 4.8 K; microwave power, 20 mW. The $g = 2$ region, which is interfered with by EPR signal IIs, is removed for clarity. The vertical dashed lines show the positions of the hyperfine lines of the modified $g = 2$ multiline EPR signal.

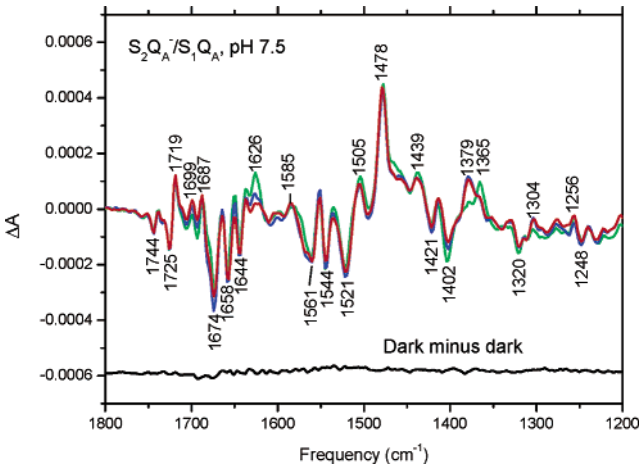

FIGURE 5: Light-minus-dark $S_2Q_A^-/S_1Q_A$ FTIR difference spectra of PSII samples with 100 mM $^{14}NH_4Cl$ (blue line), $^{15}NH_4Cl$-treated (red line), and NaCl (green line), respectively, at 250 K. Each $S_2Q_A^-/S_1Q_A$ spectrum is the average of eight to ten difference spectra. The sample suspension also included 0.1 mM DCMU. The intensity of each spectrum was normalized with respect to the Q_A^- band at 1478 cm^{-1}. The dark-minus-dark spectrum shown at the bottom is collected immediately before the light-minus-dark spectra of the $^{14}NH_4Cl$-treated PSII samples. It gives an indication of the noise level in the light-minus-dark spectrum.

might appear in the symmetric carboxylate stretching region (1450−1300 cm^{-1}) after treatment with NH_3. According to studies of ammonia inorganic compounds (*47*), we might expect to see the symmetric deformation modes of metal-bound NH_3 in this region. To test this possibility, we performed FTIR experiments on $^{15}NH_4Cl$-treated PSII samples.

Figures 5 and 6 show the $S_2Q_A^-/S_1Q_A$ FTIR difference spectra and the double-difference S_2/S_1 FTIR difference spectra of $^{14}NH_4Cl$ (blue line), $^{15}NH_4Cl$-treated (red line), and controlled (NaCl, green line) PSII samples at 250 K, respectively. The double-difference S_2/S_1 FTIR difference

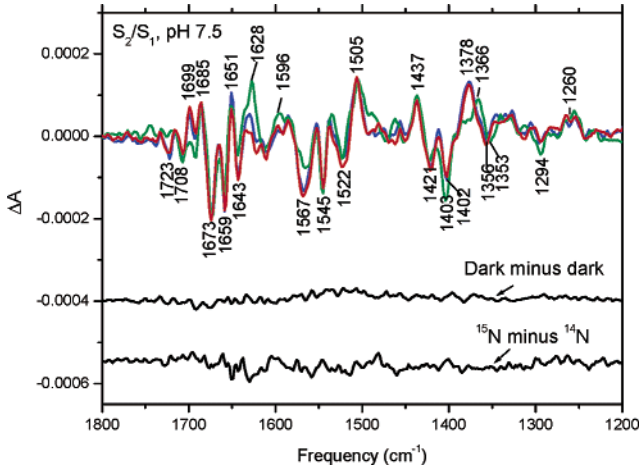

FIGURE 6: Double-difference S_2/S_1 spectra of PSII samples with 100 mM $^{14}NH_4Cl$ (blue line), $^{15}NH_4Cl$-treated (red line), or NaCl (green line) at 250 K. Each S_2/S_1 spectrum was obtained by subtracting the light-induced Q_A^-/Q_A difference spectrum from the light-minus-dark $S_2Q_A^-/S_1Q_A$ FTIR difference spectrum of PSII samples. The sample suspension included 0.1 mM DCMU for the $S_2Q_A^-/S_1Q_A$ FTIR difference spectrum or 0.1 mM DCMU and 10 mM NH_2OH for the Q_A^-/Q_A difference spectrum. The intensity of each spectrum has been normalized with respect to the Q_A^- band at 1478 cm^{-1}. The double-difference dark-minus-dark spectrum shown at the bottom was obtained by subtracting the dark-minus-dark spectrum of the Q_A^-/Q_A difference spectrum from the dark-minus-dark spectrum of the $S_2Q_A^-/S_1Q_A$ FTIR difference spectrum of $^{14}NH_4Cl$-treated PSII samples. The dark-minus-dark spectra were collected immediately before the light-minus-dark spectra of the $^{14}NH_4Cl$-treated PSII samples. It gives an indication of the noise level in the double-difference S_2/S_1 spectrum. The ^{15}N minus ^{14}N spectrum is generated by subtracting the $^{14}NH_4Cl$ S_2/S_1 spectrum from the $^{15}NH_4Cl$ S_2/S_1 spectrum. All spectra are collected at 4 cm^{-1} resolution.

spectra were obtained by subtracting the Q_A^-/Q_A FTIR difference spectrum from the $S_2Q_A^-/S_1Q_A$ FTIR difference spectrum of PSII samples (*24*, *32*, *34*). The deformation bands of metal-bound NH_3 are expected to be present at ∼1600 cm^{-1} (asymmetric) and 1400−1000 cm^{-1} (symmetric). The symmetric deformation modes of metal-bound NH_3 generally show a ^{15}N-induced shift of 2−5 cm^{-1}, and the asymmetric deformation modes generally do not show a significant ^{15}N-induced shift (*47*). As shown in Figure 6, we found no significant differences between the S_2/S_1 spectra of $^{14}NH_4Cl$ (solid line) and $^{15}NH_4Cl$-treated (dashed line) PSII samples (see the ^{15}N minus ^{14}N difference spectrum). Therefore, the spectral change in the symmetric carboxylate stretching region is unlikely due to the absorption from NH_3-derived species. We hypothesize that the symmetric deformation modes of the manganese-bound NH_3 might be too weak to be detected in our spectra. In fact, the bending modes of the manganese-bound H_2O which is expected to show up at about 1650 cm^{-1} were not identified in the S_2/S_1 FTIR difference spectrum due to their very weak extinction coefficient (*25*). Our results do indicate, however, that the S_2 carboxylate mode at 1365 cm^{-1} in the $S_2Q_A^-/S_1Q_A$ FTIR difference spectrum of controlled PSII samples at 250 K is upshifted to 1379 cm^{-1} in the spectrum of NH_3-treated PSII samples.

By comparing the S_2/S_1 spectra of the $^{14}NH_4Cl$ (blue line) and $^{15}NH_4Cl$-treated (red line) PSII samples with the spectrum of controlled (NaCl, green line) PSII samples in Figure 6, we found that the major spectral features in all

three spectra are very similar. Therefore, our result generally supports the suggestion from previous EXAFS results that the redox state of the Mn, the Mn ligand environment, and the orientation of the Mn complex are not affected by NH_3 binding to a significant extent (*18*). However, there are some significant differences in the spectral regions of the amide I (1700−1620 cm^{-1}), amide II (1570−1550 cm^{-1}), asymmetric carboxylate stretching (1640−1500 cm^{-1}), and symmetric carboxylate stretching regions (1450−1300 cm^{-1}) of the S_2/S_1 FTIR difference spectra between the NH_3-treated and controlled samples. The symmetric carboxylate stretching mode at ∼1366 cm^{-1} appears to be upshifted to ∼1378 cm^{-1} by NH_3 treatment, shown in the $S_2Q_A^-/S_1Q_A$ experiments (see above). In addition, we found that there are significant spectral differences at 1699 (+), ∼1628 (+), ∼1567 (−), ∼1403 (−), and ∼1353 cm^{-1} (−) of the S_2/S_1 FTIR difference spectra between the NH_3-treated and controlled samples. Because NH_3 is known to bind to Mn under the condition of our experiment, therefore our results suggest that there are some structural perturbations in the protein and ligand environment around the OEC when NH_3 binds to the Mn cluster during the S_1 to S_2 transition. Alternatively, these spectral differences might be caused by the difference in ionic effects of NH_4Cl vs NaCl on the PSII/OEC. For example, as shown in Figures 5 and 6, the intensity of the S_1 carboxylate mode at 1402 cm^{-1} seems to decrease in the NH_3 spectrum rather than in the controlled spectrum; however, its frequency did not significantly change. Because the intensity of the IR mode is very sensitive to environmental changes, therefore, the decrease in intensity of the S_1 carboxylate mode at 1402 cm^{-1} might be due to the difference in ionic effects of NH_4Cl vs NaCl on the PSII/OEC.

Steric Requirements of the NH_3-Binding Site in PSII/OEC. To test the steric requirements of the NH_3-binding site in PSII that gives rise to the ammonia-altered FTIR spectra, we treated the PSII samples with different primary amines (NH_3, CH_3NH_2, AEPD, and Tris) and studied them by FTIR. The results are shown in Figure 7. We found that the small amine CH_3NH_2 has a small but clear effect on the spectral change (upshift of the 1365 cm^{-1} mode) of the $S_2Q_A^-/S_1Q_A$ FTIR difference spectrum of PSII. The effects of amines on the $S_2Q_A^-/S_1Q_A$ FTIR difference spectrum (NH_3 > CH_3NH_2 > AEPD and Tris) are inversely proportional to their size (Tris ∼ AEPD > CH_3NH_2 > NH_3). However, there is no apparent correlation between the effects of amines on the $S_2Q_A^-/S_1Q_A$ FTIR difference spectrum and their pK_a value. The pK_a values (at 25 °C) of NH_3, CH_3NH_2, AEPD, and Tris are 9.2, 10.6, 9.0, and 8.0, respectively (*12*). Therefore, we conclude that this possible NH_3-binding site that gives rise to the altered $S_2Q_A^-/S_1Q_A$ FTIR difference spectra is sterically selective for small ligands. Furthermore, we found that the same effects of primary amines on the $S_2Q_A^-/S_1Q_A$ FTIR difference spectrum were observed in BBY PSII-enriched membranes (data not shown). Therefore, our results suggest that the steric requirement of the amine effect in BBY PSII-enriched membranes is very similar to that in PSII OTG cores.

Figure 8 showed the temperature dependence of the $S_2Q_A^-/S_1Q_A$ FTIR difference spectra of CH_3NH_2-treated (thick line) and controlled (thin line) PSII samples. The temperature dependence of the CH_3NH_2-induced spectral change of the

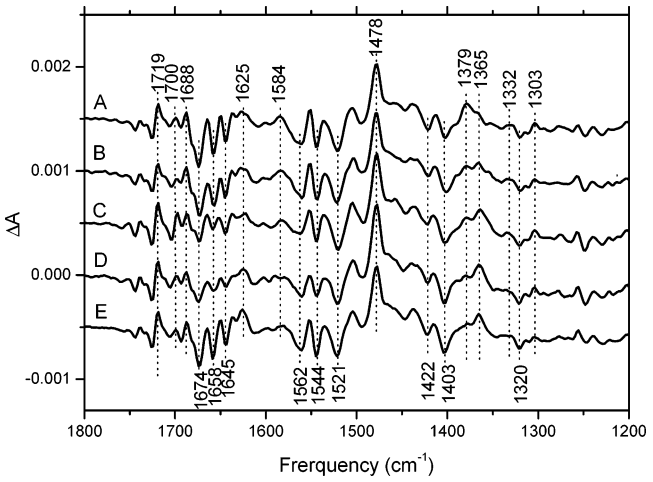

FIGURE 7: Light-minus-dark $S_2Q_A^-/S_1Q_A$ FTIR difference spectra of PSII samples with 100 mM (A) NH_4Cl, (B) CH_3NH_2, (C) AEPD, (D) Tris, and (E) NaCl, respectively. The sample suspension also included 0.1 mM DCMU. The FTIR measurement was performed at 250 K. Spectra A and E are the average of ten and eight difference spectra, respectively. The other spectra (B−D) are the average of three to four difference spectra. The intensity of each spectrum has been normalized with respect to the Q_A^- band at 1478 cm^{-1}.

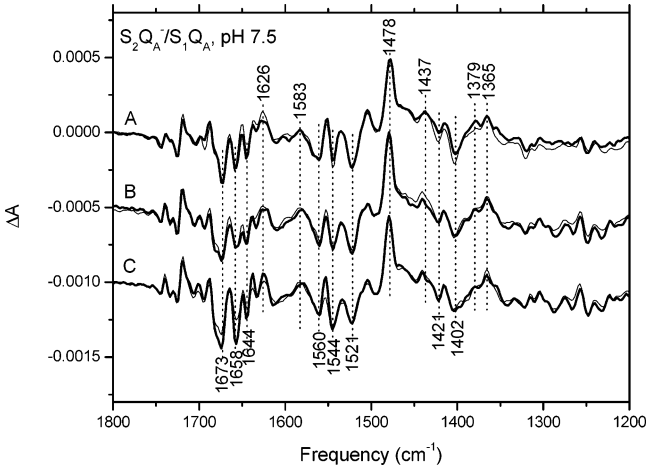

FIGURE 8: Temperature dependence of $S_2Q_A^-/S_1Q_A$ FTIR difference spectra of CH_3NH_2-treated (thick line) and controlled (thin line) PSII samples. The spectra were recorded at (A) 250 K, (B) 225 K, and (C) 200 K, respectively. The PSII samples were treated with 100 mM CH_3NH_2 or 100 mM NaCl (control). The sample suspension also included 0.1 mM DCMU. The CH_3NH_2 spectra represent the averages of two to three difference spectra. The controlled spectra represent the averages of four to eight difference spectra. The intensity of each spectrum has been normalized with respect to the Q_A^- band at 1478 cm^{-1}.

$S_2Q_A^-/S_1Q_A$ FTIR difference spectrum is very similar to NH_3 (compare to Figure 1). The intensity of the S_2 symmetric carboxylate mode at 1365 cm^{-1} was progressively decreased, and a new mode appeared in the $S_2Q_A^-/S_1Q_A$ spectrum of CH_3NH_2-treated PSII at ∼1379 cm^{-1} as the temperature of the measurement increased from 200 to 250 K.

DISCUSSION

Properties of NH_3-Binding Sites on the OEC in the S_2 State. Previous steady-state inhibition studies described two independent sites of ammonia inhibition that were named SY I and SY II (*11*, *12*). The SY I site shows inhibition by the class of amines that are competitive with Cl^-, while the SY II site is accessible only to NH_3. Previous EPR studies

identified the NH_3-specific SY II site as being located on the Mn cluster and giving rise to the S_2 state $g = 2$ NH_3-modified multiline EPR signal (*17*, *48*). These EPR studies also identified an additional NH_3-binding site on the OEC (probably SY I), not necessary on the Mn cluster, that affects the stability of the S_2 state $g = 4.1$ EPR signal (*14*, *15*, *19*−*21*). From the temperature dependence of the $g = 2$ NH_3-modified multiline EPR signal, the EPR data were interpreted as showing that NH_3 binds to the Mn cluster after the formation of the S_2 state (*13*, *19*−*21*). In this study, we found that the S_2 carboxylate mode that appears at 1365 cm^{-1} in the $S_2Q_A^-/S_1Q_A$ spectrum in controlled samples is upshifted to ∼1379 cm^{-1} upon NH_3 treatment; however, the frequency of corresponding S_1 carboxylate mode at 1402 cm^{-1} is not significantly affected (see Figures 5 and 6). These two carboxylate modes have been assigned to a Mn-ligating carboxylate whose coordination mode changes from bridging or chelating to unidentate during the S_1 to S_2 transition (*24*, *32*). Therefore, our results show that NH_3 induced a significant structural change in the OEC in the S_2 state.

Our results provide several lines of evidence in supporting that the NH_3-induced FTIR spectral changes (e.g., upshift of the 1365 cm^{-1} mode) in the $S_2Q_A^-/S_1Q_A$ FTIR difference spectrum are very likely caused by direct binding of NH_3 to the SY II site on the Mn cluster that gives rise to the altered S_2 state multiline EPR signal. First, NH_3 is known to bind to the Mn cluster under the conditions that gave rise to the NH_3-induced $g = 2$ modified multiline EPR signal. The observed correlations on the dependence of excitation temperature and NH_4Cl concentration and the steric requirement for amine effects between the NH_3-induced FTIR spectral changes (e.g., upshift of the 1365 cm^{-1} mode) in this study and the NH_3-induced $g = 2$ modified multiline EPR signal in previous EPR studies and in Figure 4 strongly suggest that these two signals very likely have the same origin. Second, the 1365 cm^{-1} mode has been assigned to be originating from an Mn-ligating carboxylate whose coordination mode changes from bridging or chelating to unidentate ligation during the S_1 to S_2 transition (*24*, *32*). The ∼12 cm^{-1} NH_3-induced upshift of the possible Mn-ligating carboxylate mode in the $S_2Q_A^-/S_1Q_A$ FTIR difference spectrum indicates that a change in structural and electronic properties of the Mn cluster has occurred under the experimental conditions. The direct binding of NH_3 to the Mn cluster could account for such a change. Third, to our knowledge, the frequency of this carboxylate mode at 1365 cm^{-1} in the $S_2Q_A^-/S_1Q_A$ FTIR difference spectrum is only affected by small amines (NH_3 and CH_3NH_2) but not significantly affected by all of the other treatments, e.g., Ca^{2+} or Cl^- depletion (*24*, *33*, *34*), substitutions with different ions (*33*, *34*), or different cryoprotectants (*29*). Therefore, this NH_3 effect (the upshift of the 1365 cm^{-1} mode) is unlikely due to the nonspecific binding of NH_3 to the OEC. Finally, our unpublished result showed that the upshift of the 1365 cm^{-1} mode in the $S_2Q_A^-/S_1Q_A$ FTIR difference spectrum was not affected by treatments with 100 mM ND_4Cl in D_2O buffer (pD 7.5). Therefore, the NH_3-induced upshift of the 1365 cm^{-1} mode in the $S_2Q_A^-/S_1Q_A$ FTIR difference spectrum is also unlikely caused by the strong hydrogen-bonding interaction between the NH_3 and the carboxylate group that gives rise to the 1365 cm^{-1} mode. On the basis of the above reasons, we proposed that the NH_3-induced FTIR spectral changes (e.g., upshift of the 1365 cm^{-1} mode) in the $S_2Q_A^-/S_1Q_A$ FTIR difference spectrum are caused by direct binding of NH_3 to the SY II site on the Mn cluster that gives rise to the altered S_2 state multiline EPR signal.

A recent FTIR study reported effects of Cl^- on S_2/S_1 difference spectra of the OEC in PSII (*34*). Their results showed that Cl^- depletion resulted in a modification of the S_2/S_1 difference spectrum. Particularly, the intensity of the S_1 carboxylate mode at ∼1404 cm^{-1} is largely suppressed, but the corresponding S_2 carboxylate mode at ∼1365 cm^{-1} is not significantly affected upon Cl^- depletion. In addition, their results also showed that the intensities of these two carboxylate modes are not affected by replacement of Cl^- with Br^-, I^-, or NO_3^-; however, both carboxylate modes are largely suppressed by the replacement of Cl^- with F^- or CH_3COO^- (*34*). The above Cl^- effects on spectral changes of the S_2/S_1 difference spectra of the OEC are dramatically different from the NH_3-induced spectral changes (e.g., upshift of the 1365 cm^{-1} mode) as shown in Figure 5. These differences show that the NH_3-induced FTIR spectral change is not caused by the displacement of Cl^- from PSII, further supporting our proposal that the NH_3-induced FTIR spectral change is caused by direct binding of NH_3 to the NH_3-specific, SY II site on the Mn cluster in PSII.

A previous study showed that amines larger than NH_3 inhibit oxygen evolution only at the Cl^- competitive SY I site (*12*). In addition, a previous EPR study has shown that amines other than NH_3 (e.g., Tris, AEPD, and CH_3NH_2) do not affect the S_2 state multiline EPR signal (*14*). The authors of these studies concluded that bulkier amines such as Tris, AEPD, and even CH_3NH_2 cannot bind to the Mn site owing to steric factors (*12*, *14*). However, as shown in Figures 7 and 8, we found that the small amine CH_3NH_2 has a small but clear effect on the spectral change (e.g., upshift of the 1365 cm^{-1} mode) of the $S_2Q_A^-/S_1Q_A$ FTIR difference spectrum of PSII. The effects of amines on the $S_2Q_A^-/S_1Q_A$ FTIR difference spectrum (NH_3 > CH_3NH_2 > AEPD and Tris) are inversely proportional to their size (Tris ∼ AEPD > CH_3NH_2 > NH_3). Furthermore, our results showed that the effects of amines on the $S_2Q_A^-/S_1Q_A$ FTIR difference spectrum in the BBYs are the same as those in the OTG RCCs. Therefore, our results suggest that the earlier EPR studies were wrong in that they would have been unable to detect small populations of PSII centers having bound CH_3NH_2 (the EPR spectra would have been dominated by the "normal" spectrum). In other words, if the NH_3-induced FTIR spectral change is caused by direct binding of NH_3 to the NH_3-specific, SY II site on the Mn cluster in PSII as we proposed, our results would suggest that the binding pocket of this NH_3-specific (SY II) site on the OEC in the S_2 state is slightly larger than the estimate from previous studies (*12*, *14*).

Previous EPR studies showed that NH_3 alters the stability of the S_2 state $g = 4.1$ EPR signals upon illumination at 200 K (*14*, *15*, *19*−*21*). These results were interpreted as showing that NH_3 binds to probably the Cl^- site (SY I) in both the S_1 and the S_2 states. In addition, it is not clear whether NH_3 binding at this site represents direct ligation to the Mn cluster or binding to a site in close proximity to the Mn cluster. As shown in Figure 1, we found that there is no apparent NH_3-induced change in the $S_2Q_A^-/S_1Q_A$ FTIR difference spectrum at 200 K. Therefore, our results indicate

that the NH_3-induced structural changes of the OEC that are responsible for the enhancement of the $g = 4.1$ EPR signal in NH_3-treated PSII samples must be small. Further studies [e.g., low-frequency FTIR (*39*−*43*), pulse EPR (*48*, *49*), resonance Raman spectroscopy (*50*, *51*), or X-ray crystallography (*7*, *8*)] will be required to identify the exact nature of the NH_3-induced structural changes of the OEC that are responsible for the enhancement of the $g = 4.1$ EPR signal and also to determine whether NH_3 binds to the Cl^- site (SY I) in both the S_1 and the S_2 states.

Because NH_3 and H_2O are similar structurally and because NH_3 inhibits photosynthetic water oxidation, the binding of NH_3 to the OEC may occur at the substrate−water binding site (*9*, *10*). CW and pulse EPR studies have provided several important structural insights into the properties of the NH_3-binding site in PSII (*13*−*23*). However, direct spectroscopic evidence proving whether any of the NH_3-binding sites (SY I or SY II) correspond to substrate H_2O-binding sites remains lacking. In this study, we found that NH_3 induced characteristic spectral changes in the region of the symmetric carboxylate stretching modes (1450−1300 cm^{-1}) of the midfrequency (1800−1200 cm^{-1}) $S_2Q_A^-/S_1Q_A$ FTIR difference spectrum of PSII. Our work demonstrates that FTIR is a potentially important tool to obtain structural information about ammonia coordination to the catalytic site of the OEC. Future FTIR studies on the high-frequency region (3500−3000 cm^{-1}) where OH vibrations of the active water and NH vibrations of NH_3 occur (*44*, *45*) and on the low-frequency region (1000−350 cm^{-1}) of FTIR difference spectra of NH_3-treated PSII samples where Mn−substrate and Mn−ligand vibrations of the OEC occur (*39*−*43*) might provide direct spectroscopic evidence to determine whether the NH_3-binding sites (SY I or SY II) correspond to substrate-binding sites in PSII and also provide other new structural insights into the S state intermediates of the OEC and the structural mechanism of photosynthetic water oxidation.

ACKNOWLEDGMENT

We are grateful to Prof. Richard J. Debus for critical reading of the manuscript. We are indebted to the reviewers for helpful comments on the manuscript.

REFERENCES

1. Barber, J. (2003) Photosystem II: the engine of life, *Q. Rev. Biophys. 36*, 71−89.
2. Debus, R. J. (2000) The polypeptides of photosystem II and their influence on mangano-tyrosyl-based oxygen evolution, in *Metal Ions in Biological Systems* (Sigel, A., and Sigel, H., Eds.) Vol. 37, pp 657−710, Marcel Dekker, New York.
3. Britt, R. D. (1996) Oxygen evolution, in *Oxygenic Photosynthesis: The Light Reactions* (Ort, D. R., and Yocum, C. F., Eds.) pp 137−164, Kluwer, Dordrecht, The Netherlands.
4. Yachandra, V. K., Sauer, K., and Klein, M. P. (1996) Manganese cluster in photosynthesis: where plants oxidize water to dioxygen, *Chem. Rev. 96*, 2927−2950.
5. Joliot, P., Barbieri, G., and Chabaud, R. (1969) Un nouveau modèle des centers photochimiques du système II, *Photochem. Photobiol. 10*, 309−329.
6. Kok, B., Forbush, B., and McGloin, M. (1970) Cooperation of charges in photosynthetic oxygen-evolution, I. A linear four step mechanism, *Photochem. Photobiol. 11*, 457−475.
7. Zouni, A., Witt, H. T., Kern, J., Fromme, P., Krauss, N., Sanger, W., and Orth, P. (2001) Crystal structure of photosystem II from *Synechococcus elongatus* at 3.8 angstrom resolution, *Nature 409*, 739−743.
8. Kamiya, N., and Shen, J.-R. (2003) Crystal structure of oxygen-evolving photosystem II from *Thermosynechococcus* vulcanus at 3.7-Å resolution, *Proc. Natl. Acad. Sci. U.S.A. 100*, 98−103.
9. Debus, R. J. (1992) The manganese and calcium ions of photosynthetic oxygen evolution, *Biochim. Biophys. Acta 1102*, 269−352.
10. Brudvig, G. W., and Beck, W. F. (1992) Oxidation−reduction and ligand-substitution reactions of the oxygen-evolving center of photosystem II, in *Manganese Redox Enzymes* (Pecoraro, V. L., Ed.) pp 119−141, VCH Publishers, New York.
11. Sandusky, P. O., and Yocum, C. F. (1984) The chloride requirement for photosynthetic oxygen-evolvtion: Analysis of the effects of chloride and other anions on amine inhibition of the oxygen-evolving complex, *Biochim. Biophys. Acta 766*, 603−611.
12. Sandusky, P. O., and Yocum, C. F. (1986) The chloride requirement for photosynthetic oxygen-evolution: factors affecting nucleophilic displacement of chloride from the oxygen-evolving complex, *Biochim. Biophys. Acta 849*, 85−93.
13. Beck, W. F., de Paula, J. C., and Brudvig, G. W. (1986) Ammonia binds to the manganese site of the O_2-evolving complex of photosystem II in the S_2 state, *J. Am. Chem. Soc. 108*, 4018−4022.
14. Beck, W. F., and Brudvig, G. W. (1986) Binding of amines to the O_2-evolving center of photosystem II, *Biochemistry 25*, 6479−6486.
15. Beck, W. F., and Brudvig, G. W. (1988) Ligand-substitution reactions of the O_2-evolving center of photosystem II, *Chem. Scr. 28A*, 93−98.
16. Britt, R. D., DeRose, V. J., Yachandra, V. K., Kim, D. K., Sauer, K., and Klein, M. P. (1990) Pulsed EPR studies of the manganese center of the oxygen-evolving complex of photosystem II, in *Current Research in Photosynthesis* (Baltscheffsky, M., Ed.) Vol. I, pp 769−772, Kluwer Academia Publishers, Dordrecht.
17. Britt, R. D., Zimmermann, J.-L., Sauer, K., and Klein, M. P. (1989) Ammonia binds to the catalytic Mn of the oxygen-evolving complex of photosystem II: evidence by electron spin−echo envelope modulation spectroscopy, *J. Am. Chem. Soc. 111*, 3522−3532.
18. Dau, H., Andrew, J. C., Roelofs, T. A., Latimer, M. J., Liang, W., Yachandra, V. K., Sauer, K., and Klein, M. P. (1995) Structural consequences of ammonia binding to the manganese center of the photosynthetic oxygen-evolving complex: An X-ray absorption spectroscopy study of isotropic and oriented photosystem II particles, *Biochemistry 34*, 5274−5287.
19. Boussac, A., Rutherford, A. W., and Styring, S. (1990) Interaction of ammonia with the water splitting enzyme of photosystem II, *Biochemistry 29*, 24−32.
20. Andréasson, L.-E., Hansson, O., and von Schenck, K. (1988) The interaction of ammonia with the photosynthetic oxygen-evolving system, *Biochim. Biophys. Acta 936*, 351−360.
21. Ono, T., and Inoue, Y. (1988) Abnormal S-state turnovers in NH_3-binding Mn centers of photosynthetic O_2 evolving system, *Arch. Biochem. Biophys. 264*, 82−92.
22. Kim, D. H., Britt, R. D., Klein, M. P., and Sauer, K. (1990) The $g = 4.1$ EPR signal of the S_2 state of the photosynthetic oxygen-evolving complex arises from a multinuclear Mn cluster, *J. Am. Chem. Soc. 112*, 9389−9391.
23. Kim, D. H., Britt, R. D., Klein, M. P., and Sauer, K. (1992) The manganese site of the photosynthetic oxygen-evolving complex probed by EPR spectroscopy of oriented photosystem II membranes: The $g = 4$ and $g = 2$ multiline signals, *Biochemistry 31*, 541−547.
24. Noguchi, T., Ono, T., and Inoue, Y. (1995) Direct detection of a carboxylate bridge between Mn and Ca^{2+} in the photosynthetic oxygen-evolving center by means of Fourier transformed infrared spectroscopy, *Biochim. Biophys. Acta 1228*, 189−200.
25. Noguchi, T., Ono, T., and Inoue, Y. (1995) A carboxylate ligand interacting with water in the oxygen-evolving center of photosystem II as revealed by Fourier transformed infrared spectroscopy, *Biochim. Biophys. Acta 1232*, 59−66.
26. Zhang, H., Razeghifard, M. R., Fischer, G., and Wydrzynski, T. (1998) Room-temperature vibrational difference spectrum for $S_2Q_B^-/S_1Q_B$ of photosystem II determined by time-resolved Fourier transform infrared spectroscopy, *Biochemistry 37*, 5511−5517.
27. Noguchi, T., Inoue, Y., and Tang, X.-S. (1997) Structural coupling between the oxygen-evolving Mn cluster and a tyrosine residue in photosystem II as revealed by Fourier transform infrared spectroscopy, *Biochemistry 36*, 14705−14711.

28. Noguchi, T., Inoue, Y., and Tang, X.-S. (1999) Structure of a histidine ligand in the photosynthetic oxygen-evolving complex as studied by light-induced Fourier transform infrared difference spectroscopy, *Biochemistry 38*, 10187−10195.
29. Onoda, K., Mino, H., Inoue, Y., and Noguchi, T. (2000) An FTIR study on the structure of the oxygen-evolving Mn-cluster of photosystem II in different spin forms of the S_2 state, *Photosynth. Res. 63*, 47−57.
30. Noguchi, T., and Sugiura, M. (2001) Flash-induced Fourier transform infrared detection of the structural changes during the S-state cycle of the oxygen-evolving complex in photosystem II, *Biochemistry 40*, 1497−1502.
31. Hillier, W., and Babcock, G. T. (2001) S-state dependent Fourier transform infrared difference spectra for the photosystem II oxygen-evolving complex, *Biochemistry 40*, 1503−1509.
32. Kimura, Y., and Ono, T.-A. (2001) Chelator-induced disappearance of carboxylate stretching vibrational modes in S_2/S_1 FTIR spectrum in oxygen-evolving complex of photosystem II, *Biochemistry 40*, 14061−14068.
33. Kimura, Y., Hasegawa, K., and Ono, T.-A. (2002) Characteristic changes of the S_2/S_1 difference FTIR spectrum induced by Ca^{2+} depletion and metal cation substitution in the photosynthetic oxygen-evolving complex, *Biochemistry 41*, 5844−5853.
34. Hasegawa, K., Kimura, Y., and Ono, T.-A. (2002) Chloride cofactor in the photosynthetic oxygen-evolving complex studied by Fourier transform infrared spectroscopy, *Biochemistry 41*, 13839−13850.
35. Noguchi, T., and Sugiura, M. (2003) Analysis of flash-induced FTIR difference spectra of the S-state cycle in the photosynthetic water-oxidizing complex by uniform ^{15}N and ^{13}C isotope labeling, *Biochemistry 42*, 6035−6042.
36. Chu, H.-A., Hillier, W., Law, N. A., Sackett, H., Haymond, S., and Babcock G. T. (2000) Light-induced FTIR difference spectroscopy of the S_2-to-S_3 state transition of the oxygen-evolving complex in photosystem II, *Biochim. Biophys. Acta 1459*, 528−532.
37. Chu, H.-A., Debus, R. J., and Babcock, G. T. (2001) D1-Asp 170 is structurally coupled to the oxygen-evolving complex in photosystem II as revealed by light-induced Fourier transform infrared difference spectroscopy, *Biochemistry 40*, 2312−2316.
38. Chu, H.-A., Hillier, W., and Debus, R. J. (2004) Evidence that the C-terminus of the D1 polypeptide of photosystem II is ligated to the manganese ion that undergoes oxidation during the S_1 to S_2 transition: An isotope-edited FTIR study, *Biochemistry 43*, 3152−3166.
39. Chu, H.-A., Gardner, M. T., O'Brien, J. P., and Babcock, G. T. (1999) Low-frequency Fourier transform infrared spectroscopy of the oxygen-evolving and quinone acceptor complexes in photosystem II, *Biochemistry 38*, 4533−4541.
40. Chu, H.-A., Gardner, M. T., Hillier, W., and Babcock, G. T. (2000) Low-frequency Fourier transform infrared spectroscopy of the oxygen-evolving complex in photosystem II, *Photosynth. Res. 66*, 57−63.
41. Chu, H.-A., Sackett, H., and Babcock, G. T. (2000) Identification of a Mn−O−Mn cluster vibrational mode of the oxygen-evolving complex in photosystem II by low-frequency FTIR spectroscopy, *Biochemistry 39*, 14371−14376.
42. Chu, H.-A., Hillier, W., Law, N. A., and Babcock, G. T. (2001) Vibrational spectroscopy of the oxygen-evolving complex and of manganese model compounds, *Biochim. Biophys. Acta 1503*, 69−82.
43. Kimura, Y., Mizusawa, N., Ishii, A., Yamanari, T., and Ono, T. (2003) Changes of low-frequency vibrational modes induced by universal ^{15}N- and ^{13}C-isotope labeling in S_2/S_1 FTIR difference spectrum of the oxygen-evolving complex, *Biochemistry 42*, 13170−13177.
44. Noguchi, T., and Sugiura, M. (2000) Structure of an active water molecule in the water-oxidizing complex of photosystem II as studied by FTIR spectroscopy, *Biochemistry 39*, 10943−10949.
45. Noguchi, T., and Sugiura, M. (2002) FTIR detection of water reactions during the flash-induced S-state cycle of the photosynthetic water-oxidizing complex, *Biochemistry 41*, 15706−15712.
46. Mishra, R. K., and Ghanotakis, D. F. (1994) Selective extraction of CP 26 and CP 29 proteins without affecting the binding of the extrinsic proteins (33, 23 and 17 kDa) and the DCMU sensitivity of a photosystem II core complex, *Photosynth. Res. 42*, 37−42.
47. Schmidt, K. H., and Muller, A. (1976) Vibrational spectra and force constants of pure amine complexes, *Coord. Chem. Rev. 19*, 41−97.
48. Peloquin, J. M., Campbell, K. A., Randall, D. W., Evanchik, M. A., Pecoraro, V. L., Armstrong, W. H., and Britt, R. D. (2000) Mn-55 ENDOR of the S-2-state multiline EPR signal of photosystem II: Implications on the structure of the tetranuclear Mn cluster, *J. Am. Chem. Soc. 122*, 10926−10942.
49. Peloquin, J. M., and Britt, R. D. (2001) EPR/ENDOR characterization of the physical and electronic structure of the OEC Mn cluster, *Biochim. Biophys. Acta 1503*, 96−111.
50. Cua, A., Stewart, D. H., Reifler, M. J., Brudvig, G. W., and Bocian, D. F. (2000) Low-frequency resonance Raman characterization of the oxygen-evolving complex of photosystem II, *J. Am. Chem. Soc. 122*, 2069−2077.
51. Cua, A., Vrettos, J. S., de Paula, J. C., Brudvig, G. W., and Bocian, D. F. (2002) Raman spectra and normal coordinate analyses of low-frequency vibrations of oxo-bridged manganese complexes, *J. Biol. Inorg. Chem. 8*, 439−451.

BI0499260